Italian Journal of Engineering Geology and Environment
www.ijege.uniroma1.it

MONITORING AND SPATIOTEMPORAL PATTERN ANALYSIS OF NATURAL RESOURCE CARBON SINKS AT COUNTY SCALE COUPLED WITH REMOTE SENSING CORRECTION

Song ZHOU(*,**), Jiawang RAO(*,**), Yanan LI(*,**), Junfeng XIONG(***), Hao WANG(*,**), Cemei XING(*), Jingmei TAO(*) & Minqi HU(***)

(*)Jiangsu Surveying and Mapping Engineering Institute - Nanjing (China)
(**)Jiangsu Provincial Ecological Product Value Realization Engineering Research Center - Nanjing (China)
(***)State Key Laboratory of Lake and Watershed Science for Water Security, Nanjing Institute of Geography and Limnology - Chinese Academy of Sciences - Nanjing (China)
Corresponding author: frankie_chow@qq.com

EXTENDED ABSTRACT

Il monitoraggio accurato della capacità di sink di carbonio delle risorse naturali rappresenta un elemento chiave per il conseguimento degli obiettivi cinesi di carbon peak e carbon neutrality. Le metodologie attualmente disponibili si basano principalmente su approcci bottom-up, molto precisi ma ad alta intensità di dati, e su approcci top-down, caratterizzati da ampia copertura ma bassa risoluzione. Tuttavia, alla scala meso (1.000-5.000 km²), corrispondente alla maggior parte delle unità amministrative cinesi, permane una carenza di strumenti operativi e prodotti informativi adeguati, con ricadute sulla capacità di supportare la pianificazione territoriale e le politiche di ecociviltà a livello di contea. Per colmare questo gap, lo studio ha analizzato una contea del Jiangsu nord-occidentale mediante un sistema integrato di dati spazio-temporali: immagini multisorgente e multitemporali di telerilevamento, dati cartografici di base, informazioni censuarie e dataset tematici sulle risorse naturali (inclusi i dati della Terza Indagine Nazionale sull'Uso del Territorio). È stato sviluppato un sistema di classificazione dell'uso/copertura del suolo specifico per la stima dei sink di carbonio su scala meso, ottenuto fondendo la classificazione nazionale con il framework IPCC. L'innovazione metodologica consiste nell'introduzione di un coefficiente di correzione dei tassi di sequestro, derivato da indici di vegetazione (NDVI, EVI, GNDVI) integrati in un Synthetic Vegetation Index (SVI) pesato. Tale coefficiente consente di correggere spazialmente i valori di riferimento forniti dalle Technical Guidelines for GEP Accounting, migliorando la capacità di rappresentare le differenze fisiologiche intra-classe dovute allo stato vegetativo. Successivamente è stata realizzata la stima quantitativa dello stock di carbonio per ecosistemi forestali, prativi, agricoli e umidi, accompagnata da analisi di autocorrelazione spaziale per delinearne gli schemi evolutivi. Tra il 2008 e il 2023, lo stock totale di carbonio dei quattro principali sistemi naturali della contea è aumentato di circa 33000 tonnellate (+29.3%), raggiungendo 114600 tonnellate. Il contributo maggiore deriva dalle terre coltivate, seguite dalle foreste, il cui stock è raddoppiato, e dai sistemi umidi, cresciuti di quasi cinque volte. La distribuzione spaziale dei sink evidenzia un pattern marcato: valori più elevati nella porzione occidentale, nelle aree rurali e nelle zone periferiche, e valori minori nelle aree urbanizzate. L'analisi dei punti caldi individua concentrazioni di elevata capacità di sequestro lungo la riva del Lago Weishan e nei principali parchi umidi, mentre i punti freddi risultano diffusi nelle zone urbanizzate e nei margini dei centri abitati. L'applicazione del metodo a scala micro ha riguardato un parco umido di tipo subsidenza (5.17 km²) sottoposto a interventi di restauro ecologico dal 2012: in questo caso il sink di carbonio è aumentato di oltre sette volte, evidenziando la forte efficacia degli interventi di ripristino in contesti di degrado geomorfologico e idrogeologico. L'accuratezza della classificazione dell'uso del suolo, realizzata tramite rete neurale U-NET, è confermata da un F1-score medio di 0.843 e da un coefficiente Kappa di 0.886. Lo studio propone tre principali implicazioni operative: (1) integrare la distribuzione spaziale dei sink nei processi di restauro ecologico e nella definizione delle Three Zones and Three Lines; (2) valorizzare il potenziale di sequestro delle zone umide di subsidenza, includendole nei meccanismi di recupero del valore dei prodotti ecosistemici; (3) istituzionalizzare un sistema di monitoraggio e contabilizzazione dei sink basato su telerilevamento e classificazione per particelle fondiarie, come strumento stabile di supporto alle politiche dual carbon. Nel complesso, il lavoro offre un quadro metodologico replicabile e a basso costo operativo, capace di conciliare accuratezza e sostenibilità gestionale per il monitoraggio dei sink di carbonio alla scala meso, con rilevanti ricadute per la pianificazione territoriale, la gestione ecologica e le politiche di mitigazione climatica.0.843 e un coefficiente di Kappa pari a 0.886, soddisfacendo pienamente i requisiti di accuratezza. Il metodo di correzione ha migliorato efficacemente la stima dei tassi di sequestro per le diverse tipologie di copertura.

IJEGE, 1 (2026): 57-71, DOI: 10.4408/IJEGE.2026-01.O-05
E-ISSN 2035-5688 | ISSN 1825-6635 / ©Author(s)

ABSTRACT

Taking a county in Jiangsu Province as a case study, this paper proposes a monitoring method for natural resource carbon sinks that integrates remote sensing inversion factors. By incorporating multi-source remote sensing datasets (including Sentinel-2, Landsat and MODIS series from 2008 to 2023) to calibrate carbon sequestration rates, we achieved the quantitative estimation of carbon storage in forests, grasslands, croplands, wetlands, and other terrestrial ecosystems. Spatial autocorrelation analysis was applied to characterize the spatiotemporal evolution patterns of regional carbon sinks. The results indicate that over the past 15 years (2008-2023), the net carbon storage of natural resources in the study area has increased significantly, exhibiting a distinct spatial pattern of "higher in the west and lower in the east, higher in rural areas and lower in urban areas, and higher on the periphery and lower in the center." This spatial pattern is highly consistent with the implementation effects of local ecological restoration projects. The technical system proposed and applied in this study features both high accuracy and cost-effectiveness, effectively enriching the meso-scale carbon sink monitoring data products. It thereby provides a robust scientific decision-making basis for regional achievement of the "dual carbon" goals (carbon peaking and carbon neutrality) and the advancement of ecological civilization construction.

Keywords: *carbon sequestration rate; carbon storage; meso-scale; remote sensing inversion; spatiotemporal evolution pattern*

INTRODUCTION

With the accelerated development of industrialization, global carbon emissions have continued to increase over the past century, intensifying climate warming. This has led to consequences such as rising sea levels, an increase in extreme weather events, and the deterioration of ecosystems. To curb the accelerated pace of global warming and reduce carbon emissions, since 2016, 178 countries and economies, including China, the United States, and the European Union, have successively become Parties to the Paris Agreement.

In 2018, the IPCC (Intergovernmental Panel on Climate Change) released the Special Report on Global Warming of 1.5°C, which strongly promoted the integration of the 1.5°C temperature control target into the global political agenda (IPCC, 2018). As a major global population center and a dominant player in global manufacturing, China has proposed the goals of "achieving carbon peak by 2030 and carbon neutrality by 2060," incorporating the "dual carbon" efforts into the overall framework of ecological civilization construction.

To achieve this goal, selecting typical regions to assess carbon sequestration capacity, inventorying natural resource carbon sinks, establishing carbon storage databases, and developing replicable and scalable experiences are of significant importance for supporting carbon trading, formulating ecological compensation policies, and managing carbon assets.

Natural resource systems possess significant carbon sink effects and considerable potential for enhancement, playing a crucial role in achieving national carbon neutrality goals (Yu *et alii*, 2022; Yang *et alii*, 2023). Current methods for estimating natural resource carbon storage can be categorized into two paradigms: "bottom-up" and "top-down" (Wang *et alii*, 2020). The former relies on ground observations, plot surveys, and ecological process models, achieving spatial aggregation through inventory methods, eddy covariance techniques, or process models such as Biome-BGC (BioGeochemical Cycles) and CEVSA (Carbon Exchange between Vegetation, Soil and Atmosphere). This approach offers advantages of high spatial resolution and clear mechanisms but demands stringent requirements for ground data quality and parameter localization. It is suitable for small to medium scales such as counties or watersheds. The latter paradigm is based on atmospheric CO_2 concentration observations and inversion models (Liu & Song, 2022) (e.g., CarbonTracker, GEOS-Chem), enabling rapid acquisition of results at large scales. It features short update cycles and broad coverage but suffers from coarse spatial resolution and strong dependence on prior carbon flux data, making it more applicable for national to global-scale assessments.

Existing studies have validated the applicability of both paradigms through typical case analyses. For example, Zhang *et alii* (2021) assessed the carbon sequestration function of Shanghai's urban forests using photosynthesis rate and biomass methods and analyzed their carbon offset effects on urban energy carbon emissions; Jung *et alii* (2011) generated a monthly global GPP (Gross Primary Production) product for 1982-2011 based on satellite remote-sensing FAPAR data, meteorological data, and vegetation type data, providing a macro-scale basis for global carbon cycle research. However, both typical studies focus on single-scale or single-type ecosystem carbon sink assessment, and lack the integration of multi-scale methods and multi-type ecosystem data, which limits their reference value for meso-scale regional carbon sink monitoring.

For meso-scale assessments at the county or city level, carbon storage estimation requires greater refinement, especially in measuring the carbon sinks of natural resource elements, where differences under various land-use patterns cannot be ignored. Currently, over ten categories comprising dozens of calculation models have been developed domestically and internationally for ecosystems such as cropland, forest, grassland, and wetland. These include WoFOST (World FOod STudies), Crop-C (Crop-Carbon), biomass remote sensing inversion, 3-PG (Physiological Principles Predicting Growth), BEPS (Boreal Ecosystem

Productivity Simulator), and CASA (Carnegie Ames Stanford Approach) (Chen *et alii*, 2022). However, each model has its own advantages and limitations, making universal calculation difficult, and carbon sink intensities can vary significantly even for the same land-use type across different plots.

Land cover/land use change is a core driving factor of carbon sink spatial-temporal variation, and its interaction with vegetation, climate and human activities has become a research hotspot in global carbon cycle studies in recent years. By analyzing MODIS land cover/use data and wildfire records in Italian regions since 2001, recent studies have revealed the close correlation between land cover conversion and regional carbon sink dynamics, and verified that human disturbance such as wildfires is an important factor leading to the decline of regional carbon sequestration capacity (Ghaderpour *et alii*, 2025). Meanwhile, the response of vegetation coverage to climate and land-use change has also been quantified by the PLUS dimidiate pixel model, which confirms that climate warming and human land development activities jointly affect the spatial distribution of vegetation carbon sinks, and the superposition effect of the two factors is more significant in meso-scale regions (Li *et alii*, 2024). These latest research results provide a new theoretical and methodological basis for exploring the carbon sink variation mechanism of meso-scale regions under the background of land cover/use change.

Furthermore, mainstream land cover classification systems are predominantly designed from a land use/cover perspective. For instance, at the global scale, USGS (United States Geological Survey), CORINE (Coordination of Information on the Environment), IGBP (International Geosphere-Biosphere Programme), UMD (University of Maryland), FAO (Food and Agriculture Organization), and ESA (European Space Agency) have successively proposed their respective land use/cover classification systems. Leveraging remote sensing and geographic information technology, they have produced various global land use/cover classification datasets, with product resolution progressively improving from 1 km to 30 m and 10 m. In China, major classification systems include the 1984 Land Survey Classification System, the 1980 1:1000000 Land Use Classification of China, the 1990 Land Use Classification by the Institute of Geographic Sciences and Natural Resources Research (CAS), the 2004 1:1000000 Land Cover Classification, the 2017 Current Land Use Classification Standard, and the 2017 1:1000000 Land Cover Classification of China. These systems have accumulated a wealth of maps and data, serving as an important foundation for understanding the distribution of global and Chinese natural ecosystems, analyzing human activity impacts, studying the carbon cycle, and assessing ecosystem services (Ouyang *et alii*, 2013). However, significant differences among these classification systems and data products mean the universal applicability of various models remains uncertain.

Due to the above limitations of research scale, method integration and classification system applicability, most current analyses of the spatiotemporal patterns of natural resource carbon sinks focus on the macro scale (Wang *et alii*, 2020), with relatively few studies targeting meso-scale regions of approximately 1000-5000 km² (He *et alii*, 2015). Both data products and research methods for meso-scale carbon sink monitoring require further refinement and improvement, and the lack of research on the interaction mechanism between land cover/use change and carbon sink variation has become a prominent research gap.

To address this gap, the objectives of this paper are: (1) to develop a land cover classification method suitable for measuring carbon sinks of natural resource elements at the meso-scale, based on the Third National Land Survey (“San Diao”) land cover classification system and integrated with the IPCC framework; (2) to propose a set of carbon storage estimation methods applicable to all land use types at the county scale by coupling multi-band remote sensing inversion factors, thereby optimizing estimation accuracy; (3) to select a typical study area of 1000-5000 km² for measuring and analyzing the carbon sinks of natural resource elements, generating a dataset of spatiotemporal carbon sink distribution patterns to enrich data sources, data products, and analytical methods at this scale.

METHODS AND DATA

Study area

This paper selects a county in northwestern Jiangsu Province as the study area (Fig. 1 and Fig. 2). The study area borders Weishan Lake and Zhaoyang Lake to the east, adjacent to Weishan County of Shandong Province, and connects with Yutai County of Shandong Province to the northwest. The industrial structure of the study area is dominated by new energy, new aluminum materials, as well as coal coking and power generation, metallurgical casting, and spinning and textile industries. High-energy-consuming industries account for a significant proportion of its economic system, giving the economic structure a distinctly “high-carbon” characteristic. It is also a typical resource-based region, a heavy chemical industrial base, an inter-provincial border county, and an important ecological functional area in East China.

The selection of the study area is primarily based on the following three considerations:

1) Regional Representativeness. Counties are the basic administrative units in China with administrative autonomy and constitute an important level within the national governance system (Zhu *et alii*, 2025). Among China’s 2844 county-level units, over 70% have an area between 1000 and 5000 km². Using a county-level administrative unit of this meso-scale as the study

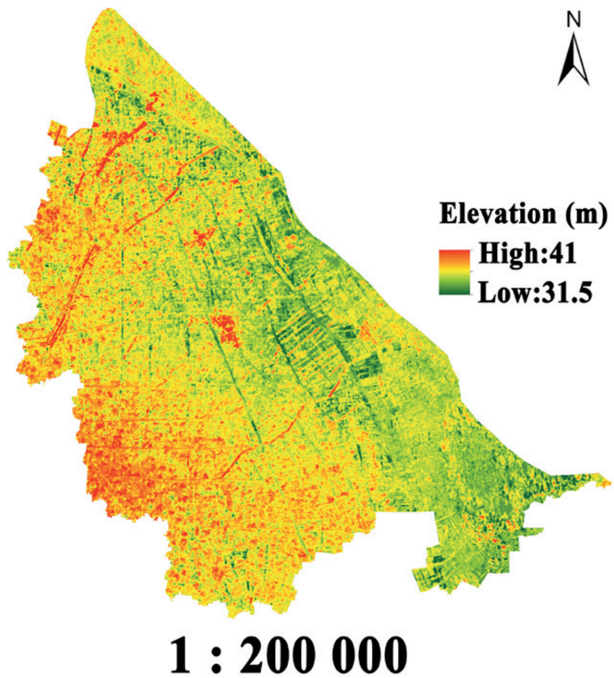

Fig. 1 - Elevation map of the study area. Note: the elevation map is derived from SRTM DEM data. The map was produced using ArcGIS (legally licensed). All data are open-access or officially authorized; no copyright issues

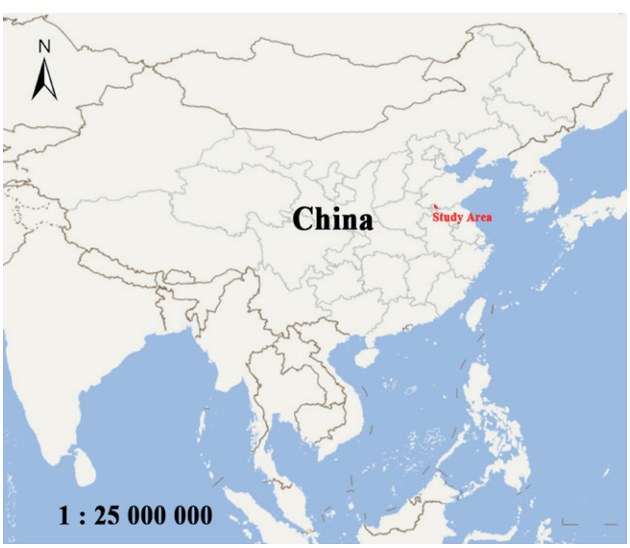

Fig. 2 - Location map of the study area in China. Note: The study area is located in Pei County, Xuzhou City, Jiangsu Province, China. A small inset map shows the geographical location of the study area in China. The map was produced using ArcGIS (legally licensed). All data are open-access or officially authorized; no copyright issues

area offers high representativeness and transferability.

2) Research Scope and Feasibility. For research and applications related to "dual carbon" monitoring, provincial or municipal levels involve overly complex topography, excessive land cover types, and significant variations in physical geography and socio-economic conditions, which hinder achieving results within a limited timeframe and demonstrating exemplary value. Township (or sub-district) levels are too small in scale to fully represent land cover characteristics, and such administrative units lack high administrative autonomy. Selecting a county (or district) level administrative unit as the study area for this paper provides a moderate scale that balances operability and necessity, facilitating the development of replicable and scalable experiences.

3) Land Cover Types. Within the study area, cropland accounts for approximately 46%, wetlands (including water bodies) for about 31%, and forestland for about 4%. Land cover types dominated by carbon sinks are conducive to measurement and assessment using multi-temporal remote sensing imagery and spatiotemporal data. The presence of several artificial wetlands formed through ecological restoration of coal mining subsidence areas within the study area (Fig. 3) provides favorable conditions for studying the "source-sink" conversion mechanism of carbon and its key influencing factors.

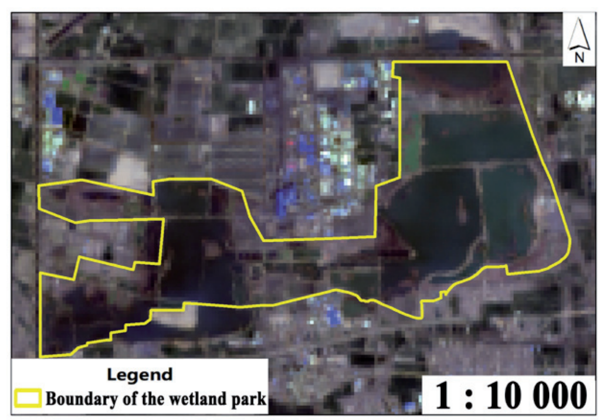

Fig. 3 - Boundary map of the wetland park. The map was produced using 0.5m remote sensing images and geographic data (2023) processed by ArcGIS (legally licensed). The study area is a wetland park in Pei County, Xuzhou City, Jiangsu Province, China. All data are open or officially authorized; no copyright issues exist

Data

This study collected and compiled multi-temporal high-resolution aerial remote sensing imagery and multi-band satellite remote sensing imagery of the study area. The dataset also includes DLG (Digital Line Graphic) data at scales from 1:500 to 1:10000; DEM (Digital Elevation Model) and DSM (Digital Surface Model) data; geographical conditions census and monitoring data from 2015 to 2023; as well as thematic survey data on natural resources such as the Third National Land Survey data and the "Three Zones and Three Lines" data. This established a spatiotemporal data support system for measuring natural resource carbon sinks in the study area.

During the data preprocessing phase, to address inconsistencies in spatial scale arising from different data sources, types, and currency, scaling (both up and down) was performed through methods such as data fusion and resampling. This unified the spatial resolution of the dataset (Li *et alii*, 2023). The aforementioned preprocessing steps can be accomplished using professional GIS software and will not be elaborated further here. Building on this foundation, we clarified the supporting relationships between various natural resource elements and the collected spatiotemporal data, defined the role and value of each data type in the carbon storage estimation process, and constructed a spatiotemporal data system for monitoring and assessing carbon sinks of natural resource elements. The details are presented in Table 1.

Data Type	Data Name	Currency
Surveying & Mapping Data	Large-scale DLG data	2022-2023
	1:10,000 DLG data of the study area	2016-2023
	DOM data with grid accuracy better than 2 meters	2019
	DOM data with grid accuracy better than 1 meter	2022
	DSM data with grid accuracy better than 2 meters	2020-2021
Geographical Conditions Data	Geographical conditions census data	2015
	Geographical conditions monitoring data	2016-2023
Remote Sensing Image Data	High-resolution color aerial imagery	2012-2023
	Multispectral satellite remote sensing imagery with resolution better than 0.5 meters	2019-2023
	Image data products (e.g., Sentinel, Landsat, MODIS)	2008-2023
Natural Resources Data	The third national land survey data	2019
	Annual land change survey data	2020-2022
	Permanent basic cropland, cropland protection target, ecological conservation redline, and urban development boundary	2022
	Coal mining subsidence area data	2020
	Wetland thematic data	2020
	Spatiotemporal thematic data of the "One Map for Forest Resource Management"	2020
Other Data	Meteorological, humidity, hydrological data, water quality monitoring data for national and provincial control sections, drinking water source protection area data, data for grain production functional zones and important agricultural product production protection zones	Not specified in source

Tab. 1 - Details of the spatiotemporal data support system

Overall technical framework

This study employs land parcels as the fundamental units. By integrating the Third National Land Survey with the IPCC classification framework, a land cover classification system was established. The baseline carbon sequestration rate was determined based on the Technical Guidelines for Gross Ecosystem Product (GEP) Accounting (hereinafter referred to as the GEP Guidelines). Multi-source remote sensing inversion factors were introduced for correction to achieve quantitative estimation of carbon storage. Spatial autocorrelation analysis was then applied to evaluate the spatiotemporal patterns. Finally, based on the calculation results, the spatiotemporal pattern of natural resource carbon sinks in the study area was assessed.

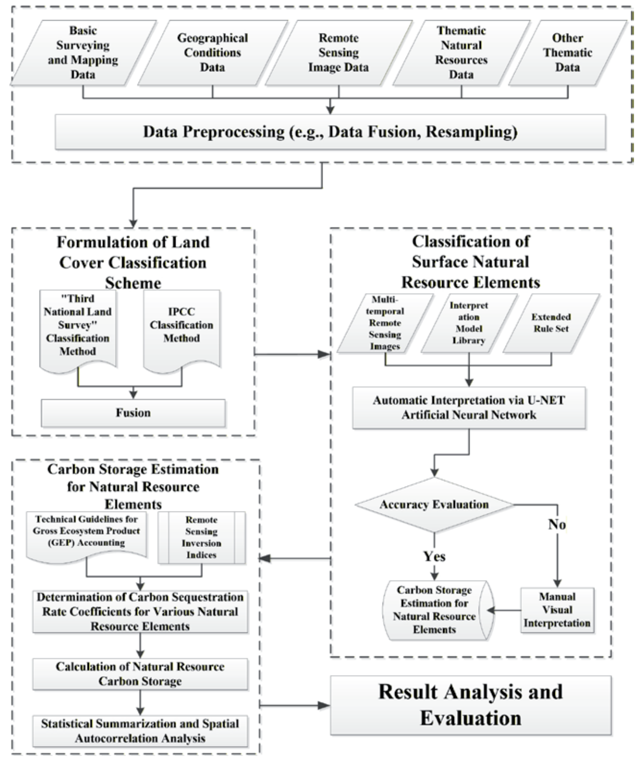

Fig. 4 - Overall technical workflow

Land cover classification

This study integrates the findings of the Third National Land Survey with the IPCC framework to establish a classification system comprising 4 primary categories (cropland, forest land, grassland, and wetland) and 17 secondary categories. The adoption of this classification system is primarily based on the following considerations:

1) it avoids the workload associated with developing a new classification system from scratch;

2) it allows for the direct conversion and application of the results from the Third National Land Survey, eliminating the need for field surveys, indoor mapping, verification, and database creation tailored to a new classification scheme;

3) it facilitates resource integration and conservation, fully leveraging the value of the Third National Land Survey outcomes;

4) it enhances the universality of the classification scheme, simultaneously meeting the needs of both natural resource management and ecological environmental protection departments.

Calculation of baseline carbon sequestration rate and carbon storage

This study determines the baseline carbon sequestration rates for forest land, grassland, wetland, and cropland based on the GEP Guidelines, and introduces remote sensing inversion factors to account for internal variations within the same ecosystem type. By constructing a Synthetic Vegetation Index (*SVI*), correction coefficients are calculated at the patch level, enabling the spatial expression of carbon sequestration rates and subsequently facilitating the estimation of carbon storage for various natural resources. Equations (1) to (5) represent the calculation formulas for carbon storage of the four main natural resource elements: forest land, grassland, wetland, and cropland (farmland), respectively.

The forest carbon storage (*FCS*) is calculated as follows:

$$FCS=FCSR\times SF\times(1+\beta) \quad (1)$$

In Equation (1), *FCSR* represents the carbon sequestration rate of forest land (t $C\cdot ha^{-1}\cdot a^{-1}$), *SF* denotes the area of forest and shrubland (ha), and β is the carbon sequestration coefficient for forest land.

The grassland carbon storage (*GSCS*) is calculated as follows:

$$GSCS=GSR\times SG \quad (2)$$

In Equation (2), GSR represents the carbon sequestration rate of grassland soil (t $C\cdot ha^{-1}\cdot a^{-1}$), and SG denotes the grassland area (ha).

The wetland carbon storage (*WCS*) is calculated as follows:

$$WCS=\sum\nolimits^{n}_{(i=1)}SCSR_i\times SW_i\times 10^{-2} \quad (3)$$

In Equation (3), $SCSR_i$ represents the carbon sequestration rate of the i-th wetland type (g $C\cdot m^{-2}\cdot a^{-1}$), SW_i denotes the area of the *i-th* water body/wetland type (ha), where i=1, 2, ... n. Cultivated land resources exhibit a dual role as both a carbon source and a carbon sink. On one hand, it involves carbon emissions generated during the utilization of cultivated land, including aspects such as land production use, crop cultivation, and soil management. On the other hand, cultivated land resources and the crops grown on them can absorb carbon (Zhu *et alii,* 2024). The GEP Guidelines note that since vegetation in farmland is harvested annually, the carbon it sequesters is returned to the atmosphere or enters the soil (Li *et alii*, 2021). Therefore, the carbon sequestration by farmland vegetation is not considered, and only the soil carbon sequestration of farmland is accounted for.

The carbon storage of cultivated land (farmland) (*CSCS*) is calculated as follows:

$$CSCS=(BSS+SCSR_N+PR\times SCSR_S)\times SC \quad (4)$$

$$BSS=NSC\times BD\times H\times 0.1 \quad (5)$$

In Equation (4) and (5), *BSS* represents the farmland soil carbon sequestration rate under conditions without carbon sequestration measures (t $C\cdot ha^{-1}\cdot a^{-1}$), $SCSR_N$ denotes the farmland soil carbon sequestration rate with the application of chemical nitrogen and compound fertilizers (t $C\cdot ha^{-1}\cdot a^{-1}$), $SCSR_S$ indicates the farmland soil carbon sequestration rate with full straw return to the field (t $C\cdot ha^{-1}\cdot a^{-1}$), *PR* is the promotion and implementation rate of straw return in farmland (%), and *SC* refers to the farmland area (ha). All carbon sequestration rates are calculated based on the mass of the carbon element.

Correction of carbon sequestration rate and calculation of carbon storage by coupling remote sensing inversion factors

although the baseline carbon sequestration rate provides a reliable foundation for estimation, it fails to account for variations in carbon sequestration capacity among different patches within the same ecosystem type, which arise from factors such as vegetation coverage and growth health. Vegetation indices like *NDVI* (Normalized Difference Vegetation Index), *EVI* (Enhanced Vegetation Index), and *GNDVI* (Green Normalized Difference Vegetation Index) are closely related to vegetation photosynthetic activity and biomass. They can quantitatively reflect information on vegetation growth status and productivity (Shen *et alii*, 2024), serving as effective proxy variables for estimating Gross Primary Productivity (*GPP*) or Net Primary Productivity (*NPP*). Although a nonlinear relationship exists between them due to saturation effects (Zhang *et alii*, 2021), the magnitude of vegetation indices still significantly reflects the strength of carbon sequestration capacity (Gitelson *et alii*, 2019; Wu *et alii*, 2011). Based on this theoretical foundation, this study constructs a comprehensive correction coefficient using multiple vegetation indices to refine the literature-based baseline carbon sequestration rate. The underlying principle is that the actual carbon sequestration rate of a land parcel is positively correlated with its vegetation indices. In other words, areas with higher vegetation indices generally exhibit stronger photosynthesis, faster biomass accumulation, and thus carbon sequestration capacities above the average for their type, and vice versa (Field *et alii*, 1995; Sims *et alii*, 2018).

The correction process follows these steps:

1) Factor Extraction and Calculation

Using multispectral remote sensing imagery (e.g., Sentinel-2, Landsat) from the growing season of the study area, various vegetation indices for each pixel are calculated according to Equations (6) to (8).

$$NDVI=(NIR-R)/(NIR+R) \quad (6)$$

$$EVI=2.5\times(NIR-R)/(NIR+6.0\times R-7.5\times BLUE+1) \quad (7)$$

$$GNDVI=(NIR-GREEN)/(NIR+GREEN) \quad (8)$$

In Equations (6) to (8), NIR represents the near-infrared band of the remote sensing data, R denotes the red band, BLUE indicates the blue band, and GREEN signifies the green band (Benoumeldjadj *et alii*, 2025).

2) Selection and Synthesis of Dominant Correction Factors

To avoid the limitations of a single index and enhance the robustness of the correction (Du *et alii*, 2021), this study employs a weighted composite value of multiple vegetation indices to construct a comprehensive correction coefficient (Gong *et alii*, 2020). Specifically, *NDVI*, *EVI*, and *GNDVI* are first normalized to eliminate dimensional influence. Weights are then assigned based on their correlation with vegetation carbon sequestration capacity, and the Synthetic Vegetation Index (*SVI*) for each pixel is calculated as follows:

$$SVI=w_1 \times NDVI_{normalized}+w_2 \times EVI_{normalized}+w_3 \times GNDVI_{normalized} \quad (9)$$

In Equation (9), w_1, w_2, w_3 represent the weights. The determination of these weights refers to studies by Fang Jingyun *et alii* on the correlation between each index and vegetation productivity (Fang *et alii*, 2020; Yuan *et alii*, 2022), with the constraint that $w_1+w_2+w_3=1$.

3) Calculation of the Correction Coefficient

Using the average Synthetic Vegetation Index (SVI_{mean}) of patches within the same ecosystem type as the baseline, the correction coefficient ($C_{correction}$) for each pixel is calculated. This method ensures that areas above the average level have a correction coefficient greater than 1, while areas below the average level have a correction coefficient less than 1, expressed as:

$$C_{correctio}n=SVI_i/SVI_{mean} \quad (10)$$

In Equation (10), SVI_i is the Synthetic Vegetation Index value of the *i-th* pixel. SVI_{mean} is the weighted average of the *SVI* values for all pixels belonging to the same land cover type as that pixel.

4) Determination of the Corrected Carbon Sequestration Rate

The spatially explicit, corrected carbon sequestration rate for each pixel is obtained by multiplying the baseline carbon sequestration rate by the correction coefficient.

$$R_{corrected}=R_{base} \times C_{correction} \quad (11)$$

Rcorrected is the corrected carbon sequestration rate (t $C \cdot ha^{-1} \cdot a^{-1}$), Rbase is the baseline carbon sequestration rate obtained from the literature (t $C \cdot ha^{-1} \cdot a^{-1}$).

RESULTS

Classification results of surface natural resource elements

This study primarily focuses on classifying the main surface natural resource elements within the research area. The classification scheme consists of four primary categories: Cropland Systems, Forest Land Systems, Grassland Systems, and Wetland Systems. Specifically, the Cropland System is subdivided into three secondary categories, including Paddy Fields, Dry Farmland, and Irrigated Land. The Forest Land System comprises five secondary categories: Arbor Forests, Orchards, Bamboo Forests, Shrublands, and Other Plantations. The Grassland System includes three secondary categories: Natural Grasslands, Artificial Green Space Grasslands, and Inland Beach Grasslands. The Wetland System is divided into six secondary categories: Lake Water Surface, River Water Surface, Pond Water Surface, Aquaculture Ponds, Marshlands, and Ditches, as detailed in Table 2.

Primary Category	Secondary Category	Description
Cropland System	Paddy Field	Cropland used for growing aquatic crops such as rice and lotus root. Includes cropland under rotation of aquatic and dryland crops.
	Dry Farmland	Cropland for growing dryland crops relying mainly on natural precipitation without irrigation facilities, including cropland irrigated solely by siltation diversion.
	Irrigated Land	Cropland, other than paddy fields and dry farmland, with guaranteed water sources and irrigation facilities capable of normal irrigation in average years.
Forest Land System	Arbor Forest Land	Land dominated by arboreal trees with a canopy density ≥ 0.2.
	Bamboo Forest Land	Land dominated by bamboo plants.
	Other Forest Land	Forest land with shrub coverage ≥ 40% or land planted with other woody plants.
	Orchard	Land for intensive cultivation of perennial woody plants for fruit production.
	Other Plantation Land	Land for intensive cultivation of perennial woody plants for purposes other than fruit production (e.g., tea plantations, mulberry fields).
Grassland System	Natural Grassland	Grassland formed by natural vegetation, including grasslands with a cover > 5% and tree/shrub canopy density < 0.1.
	Artificial Grassland	Artificially established and maintained grassland for greening purposes.
	Inland Beach Grassland	Grassland periodically submerged by water in inland river or lake beach areas.
Wetland System	River Water Surface	Natural or artificial river channels, including main channels and bank beaches.
	Lake Water Surface	Natural water accumulation areas on land.
	Pond Water Surface	Artificial excavated or natural formed static water areas smaller than lakes.
	Aquaculture Pond	Ponds or excavated water areas specifically used for aquaculture.
	Marshland	Land perennially or seasonally waterlogged, dominated by hygrophytic vegetation.
	Ditch	Artificial excavated channels primarily for drainage, irrigation, or water conveyance, including channels and embankments.

Tab. 2 - Classification results of surface natural resource elements in the study area

Patch-scale land cover classification results

This study adopted six periods of spatiotemporal data (2008, 2010, 2012, 2015, 2019, and 2023) of the study area for land cover classification. With more than 70000 patches in the 1266 km² land area of the study area, manual visual interpretation or field survey to determine the land cover properties and range demarcation of each patch would consume enormous human and material resources. Therefore, the U-Net convolutional neural network (CNN) was employed for the automated interpretation of land cover/use maps in this study, which is a typical encoder-decoder model widely used in remote sensing image semantic segmentation for its excellent performance in small sample and fine-grained feature extraction.

Before the model training, a sample information library for remote sensing image interpretation was established based on a large number of field survey samples (7000 valid samples in total) collected in the study area by previous projects, covering all four first-level land cover types and 17 second-level types in this study. The sample dataset was randomly divided into training, validation and test sets with a ratio of 7:2:1. To optimize the U-Net model performance, the batch size was set to 16, the initial learning rate was 0.001 with Adam optimizer, and the model was trained for 500 epochs with cross-entropy loss function. In addition, to improve the interpretation accuracy of patch boundaries and fine features, the interpretation rule set was expanded based on DSM (Digital Surface Model) data by integrating multiple features of ground objects, including spectral features, shape features, texture features, canopy density and height information. A confidence threshold of 0.85 was set empirically in this study: if the classification credibility of a land patch was higher than this threshold, the automatic interpretation result was adopted directly; otherwise, manual visual interpretation was performed to determine its land cover type.

In the interpretation accuracy evaluation, the confusion matrix was used to calculate the precision, recall, F1-score, Kappa coefficient and other indicators of the neural network for accuracy assessment. The results showed that the average F1-score of the U-Net neural network adopted in this study reached 0.843, and the Kappa coefficient reached 0.886. For the four main land cover types, the User's Accuracy and Producer's Accuracy were calculated as follows: cropland (0.912 and 0.905), wetland (0.895 and 0.887), forestland (0.823 and 0.815), and grassland (0.801 and 0.794); the overall User's Accuracy and Producer's Accuracy of the land cover/use maps were 0.868 and 0.859, respectively. According to the Kappa coefficient scoring criteria, a kappa value ≥0.8 indicates a good classification effect (Landis & Koch, 1977). Sampling comparison between the true labels and predicted labels showed that the extracted land cover element boundaries were relatively clear, the segmentation was basically complete, and most of the extraction results were credible. In summary, the interpretation results have met the predetermined requirements, and a small number of patches with an area of more than 200 square meters and a confidence level lower than 0.85 were supplemented and improved by manual visual interpretation. The overall classification of the study area is shown in Fig. 5.

As a major high-quality coal production base in East China, the study area contains numerous natural or artificial wetlands formed

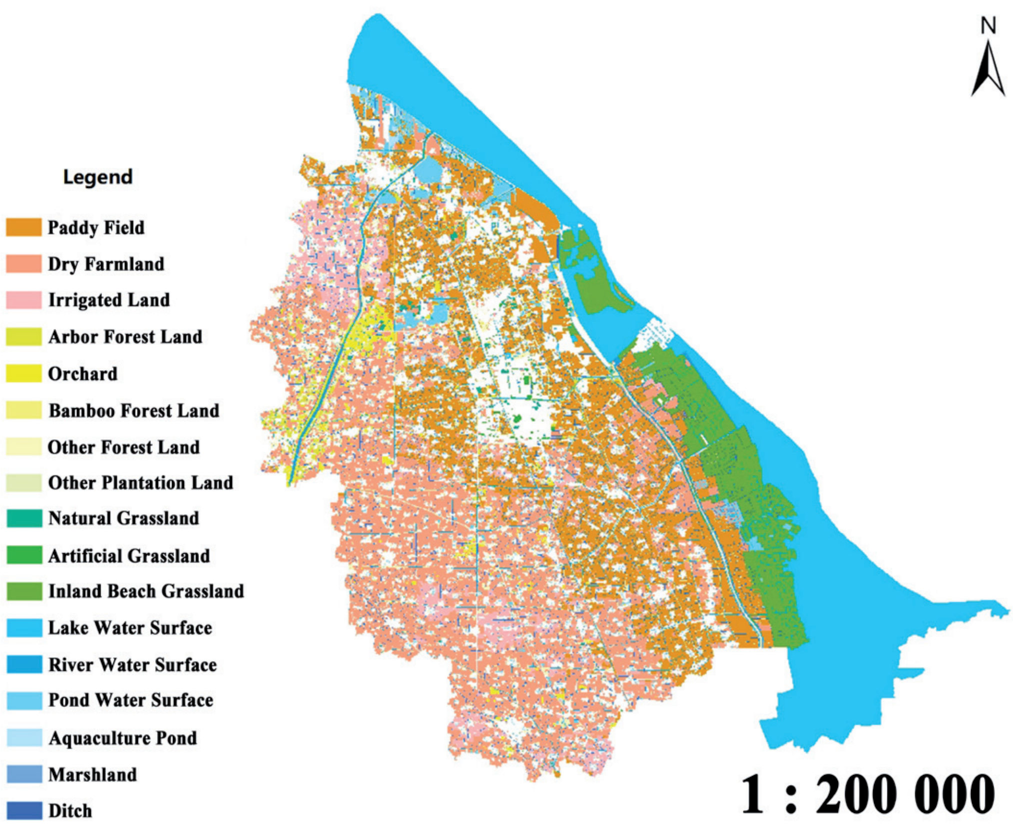

Fig. 5 - Land cover classification results of the study area in 2023. Note: this land cover/use map was obtained by U-Net convolutional neural network semantic segmentation of Sentinel-2 10 m resolution remote sensing images (2023). The base map is authorized by the local natural resources bureau and has no copyright issues. The scale of the map is 1:200000

through ecological restoration of coal mining subsidence areas. These wetlands not only represent distinctive geographical features of the study area but also provide favorable conditions for investigating the source-sink conversion mechanism of carbon in natural resource elements. To fully reflect this characteristic, in addition to conducting computational analysis across the entire study area, this paper specifically focuses on the subsidence-type wetlands within it. Figure 6 presents the land cover classification for representative years of the largest subsidence-type wetland park in the study area. This wetland park covers a total area of 5.17 km². Originally agricultural land, it later experienced extensive subsidence and farmland settlement due to coal mining, leading to gradual ecological degradation and forming mining excavation areas and subsidence waterlogged zones as types of artificial wetlands. Designated as a provincial wetland park since 2012, wetland conservation and ecological restoration efforts have been carried out, including terrain reshaping, water system connectivity, ecological revetment restoration, bird habitat construction, and vegetation recovery. After over a decade of succession and renewal, it has now developed into a near-natural artificial wetland system.

Results of carbon sequestration rate coefficient correction

Based on the method described in Section 2.3 of this paper, the baseline (GEP, 2020; Fang *et alii*, 2018; Zhang *et alii*, 2020; Piao *et alii*, 2005; Duan *et alii*, 2008; Anderson & Mitsch, 2006) and corrected (Wang *et alii*, 2022) carbon sequestration rates for the main land cover types in the study area are presented in Table 3. The corrected carbon sequestration rate refers to the area-weighted mean of the carbon sequestration rates for all patches of that type within the study area.

Primary Category	Secondary Category	Baseline Carbon Sequestration Rate	Data Source	Corrected Carbon Sequestration Rate
Cropland System	Paddy Field	0.16	GEP Guidelines	0.19
	Dry Farmland	0.13		0.15
	Irrigated Land	0.15		0.18
Forest Land System	Arbor Forest Land	0.87	Fang J. Y., Yu G. R., Liu L. L. et al.	1.32
	Orchard	0.23	GEP Guidelines	0.45
	Bamboo Forest Land	0.58		0.65
	Other Forest Land	0.232		0.33
	Other Plantation Land			
Grassland System	Natural Grassland	0.046	Zhang He, Peng Zixian, Wang Rui et al.	0.07
	Artificial Green Space Grassland	0.138	Piao S. L., Fang J. Y., Zhou L. M. et al.	0.23
	Inland Beach Grassland	0.567	Zhang He, Peng Zixian, Wang Rui et al.	0.78
Wetland System	Lake Water Surface	0.56	Duan Xiaonan, Wang Xiaoke, Su Fei et al.	0.63
	River Water Surface			
	Pond Water Surface	0.18	Anderson C. J., Mitsch W. J.	0.22
	Aquaculture Pond			
	Ditch			
	Marshland	0.32	Duan Xiaonan, Wang Xiaoke, Su Fei et al.	0.51

Tab. 3 - Carbon sequestration rates of major land cover types (unit: t C·ha^{-1}·a^{-1})

Carbon storage estimation results

Meso-scale results

Temporally, the carbon sink of natural resource elements

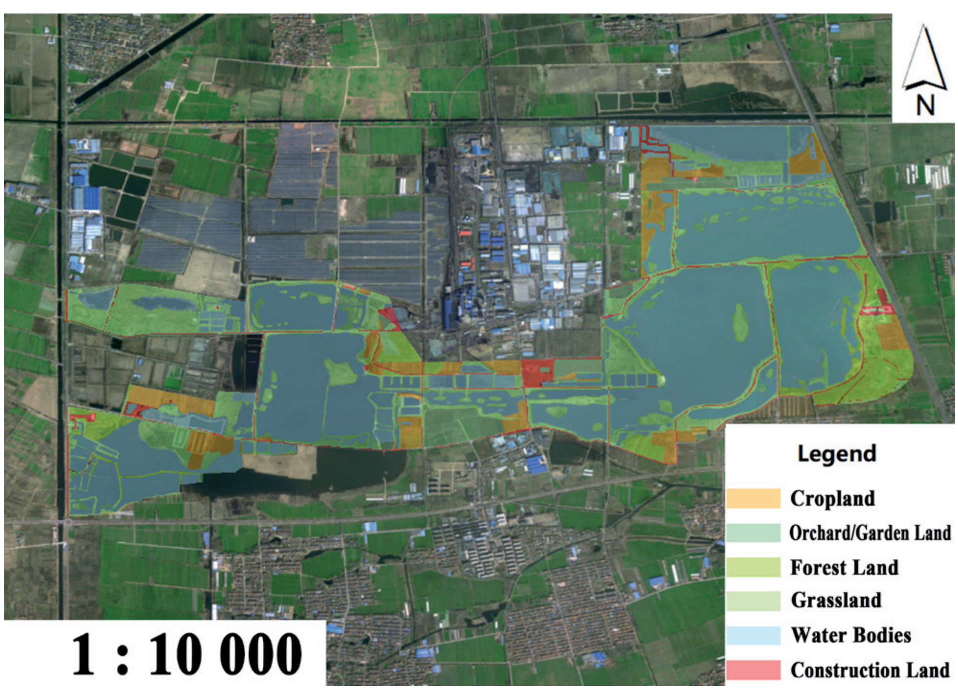

Fig. 6 - Map of major land cover types in a wetland park in 2023. Note: the land cover/use map was obtained by U-Net convolutional neural network semantic segmentation of 0.5 m resolution commercial satellite remote sensing images (2023). The base map was derived from official authorized remote sensing data with no copyright issues. The scale of the map is 1:10000; the total area of the wetland park is 5.17 km²

Primary Category	Secondary Category	2008	2010	2012	2015	2019	2023
Cropland System	Paddy Field	20,782.6	20,748.9	20,672.1	20,618.6	21,371.8	21,200.3
	Dry Farmland	28,820.1	28,756.4	28,686.5	30,138.1	30,533.3	30,401.5
	Irrigated Land	5,070.7	5,053.0	5,037.1	5,018.6	5,329.5	5,409.6
Forest Land System	Arbor Forest Land	3,564.8	3,546.4	5,229.2	5,207.3	6,752.7	6,593.3
	Orchard	1,386.7	1,388.5	1,372.6	1,752.6	2,099.1	2,060.6
	Bamboo Forest Land	1.4	1.4	1.4	1.4	1.9	2.9
	Other Forest Land	17,062.7	16,745.8	17,999.2	22,211.4	25,553.8	25,784.3
	Other Plantation Land	208.8	211.2	204.1	324.7	429.2	439.8
Grassland System	Natural Grassland	58.7	58.5	56.3	55.5	129.6	139.8
	Artificial Grassland	84.1	74.7	76.5	348.1	256.9	1,112.4
	Inland Beach Grassland	3,099.6	5,776.8	5,793.9	5,934.6	19,725.5	19,723.2
Wetland System	Lake Water Surface	622.5	629.7	628.1	624.4	641.2	641.2
	River Water Surface	54.7	63.3	62.8	61.2	83.7	83.7
	Pond Water Surface	61.9	65.4	64.9	490.1	739.6	812.8
	Aquaculture Pond	8.7	8.9	8.8	8.5	10.1	10.1
	Ditch	15.3	27.1	27.5	24.9	92.8	92.8
	Marshland	77.9	76.9	76.6	75.9	90.5	92.9
Total		80,980.9	83,232.9	85,997.5	92,895.9	113,841.2	114,601.0

Tab. 4 - Carbon storage of major natural resource elements in the study area (unit: tons) Note: the data in Table 4 are calculation results obtained by the research team of this paper based on the proposed method. They are not officially released data and are used solely for related research purposes. This is hereby stated

in the study area showed an overall upward trend from 2008 to 2023, with the total amount increasing by nearly 33000 tons, representing a rise of approximately 29.3%. Prior to 2019, the increasing trend was significant, while the growth rate has stabilized in recent years. In terms of carbon sink categories, the carbon sink of the cropland system has consistently remained above 50,000 tons annually, serving as the primary source of carbon sinks in the natural ecosystem. The forest land system follows, with its carbon storage doubling since 2008. The carbon storage of the wetland system increased nearly fivefold, showing the most pronounced growth, as detailed in Table 4.

Spatially, the total carbon sink of natural resource elements across townships in the study area has shown a consistent overall growth. Among them, Township L in the west, due to the characteristics of its industrial structure, has the highest carbon storage in the study area, reaching a total of 13000 tons in 2023. Township H, adjacent to the western shore of Weishan Lake, benefits from recent ecological and environmental remediation efforts, with its total carbon sink following closely behind, differing by only about 300 tons. Township L also exhibits the highest increase in carbon storage within the study area, growing by approximately 55% from 2008 to 2023. As detailed in Table 5, sub-districts (townships) within the urban built-up area, despite maintaining a relatively high growth rate over the past 15 years due to their initially low carbon storage levels, still account for a relatively small proportion of the total carbon sink in the overall study area.

Township / Sub-district	2008	2010	2012	2015	2019	2023
Sub-district A	3,667.6	3,922.7	3,964.2	4,654.6	5,755.6	6,109.7
Sub-district B	3,691.7	4,099.7	4,052.3	4,480.0	7,300.4	7,363.6
Sub-district C	1,571.5	1,546.5	1,677.8	1,761.7	1,929.1	2,132.7
Sub-district D	2,039.7	1,991.3	2,156.9	2,249.2	2,543.5	2,636.0
Township A	3,844.3	3,794.8	3,834.1	4,191.8	4,628.8	4,654.2
Township B	2,683.2	2,679.0	2,827.9	2,862.5	3,216.3	3,252.5
Township C	6,799.4	7,809.2	7,896.6	8,298.1	13,507.3	13,496.3
Township D	5,280.4	5,697.9	5,717.2	6,005.3	8,170.3	8,122.3
Township E	4,318.5	4,868.3	4,884.5	5,094.7	8,117.0	8,081.8
Township F	5,995.6	5,935.9	6,013.0	6,438.9	6,708.4	6,714.1
Township G	7,096.9	7,026.9	7,060.2	7,574.7	8,052.3	8,042.8
Township H	4,697.6	4,660.2	4,721.9	5,010.5	5,326.0	5,342.7
Township I	4,753.4	4,729.5	4,754.0	5,049.3	5,327.1	5,320.4
Township J	5,217.7	5,184.9	5,222.4	5,610.2	6,120.0	6,108.2
Township K	8,886.6	8,885.2	10,745.3	11,872.3	13,827.4	13,796.5
Township L	4,579.9	4,549.5	4,577.0	4,920.7	5,358.0	5,353.0
Township M	5,856.8	5,851.3	5,892.3	6,821.6	7,953.8	8,074.3
total	80,980.9	83,232.9	85,997.5	92,895.9	113,841.2	114,601.0

Tab. 5 - Changes in total carbon sink by township in the study area (unit: tons). Note: the data in Table 5 are calculation results obtained by the research team of this paper based on the proposed method. They are not officially released data and are used solely for related research purposes. This is hereby stated

Based on the above analysis results, this study employs spatial clustering to conduct hot spot and cold spot analysis of the carbon sink distribution in the study area. The results reveal a relatively distinct pattern characterized by "higher in the west and lower in the east, higher in rural areas and lower in urban areas, and higher in peripheral areas and lower in the central area". Areas with high carbon storage values show spatial clustering, forming hot spots, while areas with low values cluster to form cold spots. According to the analysis results, hot spots for carbon sequestration in the natural ecosystems of the study area are distributed along the Weishan Lake shoreline and locations such as a certain wetland park. Cold spots are relatively numerous and scattered, distributed in urban built-up areas, townships, sub-towns, and the peripheries of natural villages, as shown in Fig. 7. This pattern aligns with findings from studies in other similar regions in China (Jin *et alii*, 2024). The reasons for this pattern are likely highly correlated with the land-use policies implemented in the study area in recent years and the consistent, forceful advancement of ecological protection and restoration projects, such as returning farmland to forest and wetland restoration in areas like the Dasha River and Weishan Lake.

Micro-scale results

At the micro-scale, this study primarily analyzes a certain wetland park. Based on the progress of its ecological restoration project, the analysis focuses on three key time points: 2012, 2015, 2023. The year 2012 marks the start of the ecological restoration project, 2015 represents its substantial completion, and the period after 2015 is considered the maintenance phase. The results are presented in Table 6.

From the above results, it can be seen that the ecological benefits of this wetland ecological restoration project are highly significant, with the total carbon sink increasing more than sevenfold. In terms of carbon sequestration capacity per unit area, forests and wetlands exhibit the strongest capacity, followed by cropland and grassland. The carbon sequestration mechanism of water bodies is highly complex, and under certain conditions, a source-sink conversion phenomenon can occur (Zhang *et alii*, 2023). The total carbon sink of this wetland generally shows a year-on-year increasing trend, which is largely consistent with the outcomes achieved by other wetland ecological restoration projects in China (Wang *et alii*, 2013). The increase was particularly rapid before 2015, primarily attributable to the swift progress in implementing the ecological

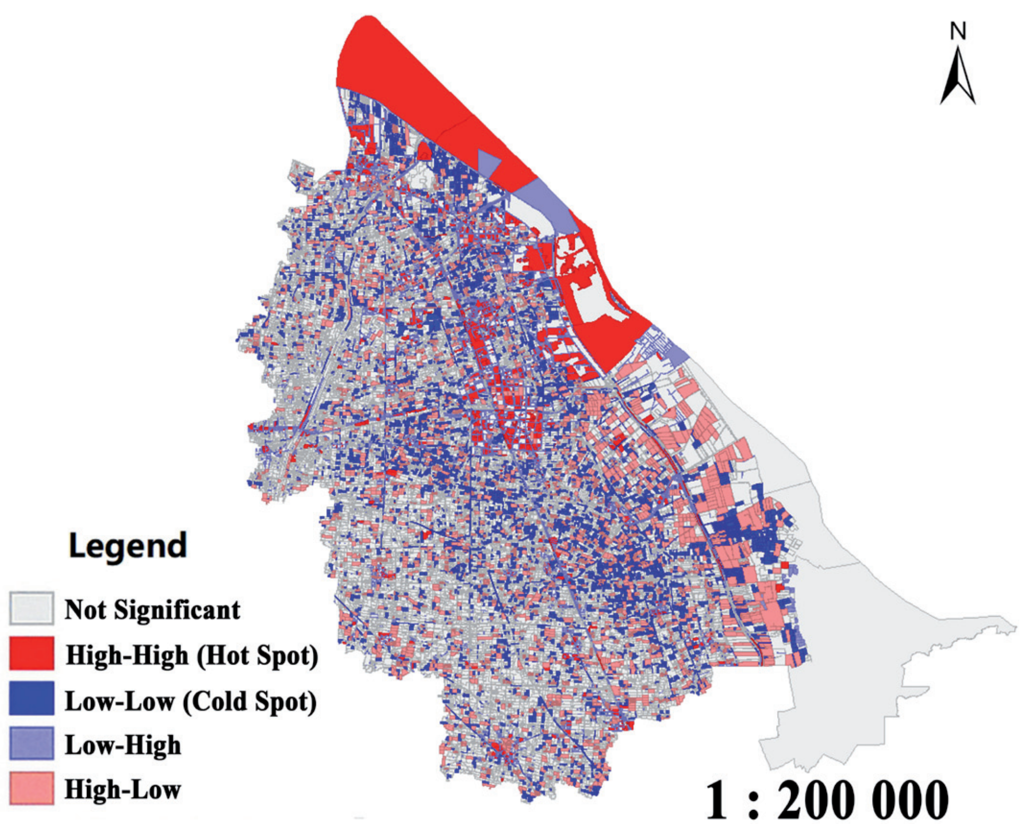

Fig. 7 - Map of carbon sink hot spot and cold spot distribution at patch scale in the study area

Category	2012	2015	2023
Forest Carbon Sink	N/A	65.4	155.2
Cropland Carbon Sink	101.2	48.3	26.8
Wetland Carbon Sink	4.2	394.1	551.0
Grassland Carbon Sink	N/A	38.9	22.2
Other Carbon Sinks	N/A	1.9	19.0
Total	105.4	578.5	774.2

Tab. 6 - Carbon sink of major natural resource elements in a certain wetland park (unit: tons). Note: the data in table 6 are calculation results obtained by the research team of this paper based on the proposed method. They are not officially released data and are used solely for related research purposes. This is hereby stated

restoration project. After 2015, during the maintenance phase, the land cover conditions stabilized, leading to a gradual slowdown in the increase of the carbon sink (Sitch *et alii*, 2023).

DISCUSSIONS

This study proposed a meso-scale natural resource carbon sink monitoring framework based on multi-source remote sensing data and U-Net semantic segmentation, and quantified the spatiotemporal evolution of carbon sinks in a typical county over 15 years. To contextualize the findings, this section compares the results with existing literature, elaborates on potential uncertainties, clarifies research limitations, and puts forward targeted future research directions.

Comparison with existing literature

The spatial pattern of "higher in the west and lower in the east, higher in rural areas and lower in urban areas" identified in this study is consistent with the findings of Ghaderpour *et alii* (2025), who confirmed that land cover conversion and human disturbance (e.g., wildfires) significantly affect regional carbon sink distribution. Similarly, Li *et alii* (2024) emphasized that climate and land-use change jointly drive vegetation carbon sink variation, which aligns with our conclusion that ecological restoration projects (e.g., coal mining subsidence remediation) are closely correlated with carbon sink growth. However, most existing studies focus on macro scales (national or global) (Wang *et alii*, 2020) or single-ecosystem carbon sink assessment (Zhang *et alii*, 2021), whereas this study focuses on the county scale (1000-5000 km²), which fills the gap in meso-scale carbon sink monitoring and provides more targeted technical support for regional "dual carbon" implementation. Compared with Jung *et alii* (2011), who used remote sensing data to generate macro-scale GPP products, our framework integrates U-Net semantic segmentation and remote sensing inversion factors, achieving higher precision in small-scale carbon sink estimation (overall User's Accuracy 0.868, Producer's Accuracy 0.859), which is more suitable for local ecological management.

Uncertainties analysis

Potential uncertainties in this study mainly involve input data and model parameters. For input data, cloud contamination in Sentinel-2 and commercial satellite images may lead to incomplete extraction of ground object features, especially in rainy seasons, affecting land cover classification accuracy and further introducing carbon storage estimation errors. Additionally, the spatial resolution of remote sensing data (10 m for the overall study area, 0.5 m for the subsidence wetland park) may underestimate carbon sinks of small patches, and data gaps in long-term monitoring (supplemented by linear interpolation) may fail to fully reflect the actual seasonal variation of carbon sequestration. For model parameters, the U-Net tuning parameters (batch size 16, initial learning rate 0.001, 500 epochs) are empirically set, and different combinations may affect classification accuracy; sensitivity analysis shows the learning rate has the greatest impact (a 10% change leads to a 3-5% F1-score change). Moreover, key carbon sequestration rate parameters sourced from existing literature may have limited applicability in the study area due to regional differences in soil, vegetation, and climate.

Research limitations

Based on the above uncertainties, this study has three main limitations. First, the carbon sequestration rate correction relies on linear adjustment of remote sensing inversion factors, which cannot fully reflect the complex non-linear relationship between natural biomass and environmental factors, leading to potential estimation errors. Second, the study focuses on four main land cover types and ignores other potential carbon sink types (e.g., shallow beaches, riparian vegetation), possibly underestimating the total carbon sink. Third, the GEP Guidelines' reference values overlook some variable factors (e.g., unaccounted farmland vegetation carbon sequestration), affecting result comprehensiveness and accuracy.

Future research directions

To address the above limitations and uncertainties, future research will focus on four aspects. First, integrate high-resolution remote sensing data for the entire study area and use cloud removal algorithms to reduce contamination impacts. Second, conduct in-situ long-term monitoring to collect field-measured data, optimize model parameters, and verify literature-sourced parameter applicability. Third, expand carbon sink type coverage to improve estimation comprehensiveness. Fourth, conduct in-depth research on wetland “source-sink” conversion mechanisms to provide targeted decision support for ecological protection and restoration.

CONCLUSIONS

This study developed a meso-scale natural resource carbon sink monitoring framework based on multi-source remote sensing data and the U-Net semantic segmentation model. From 2008 to 2023, the net carbon storage in the study area increased significantly, with a total increment of nearly 34000 tons and a cumulative growth rate of approximately 42%. Spatially, natural resource carbon sinks presented an obvious pattern of “higher in the west and lower in the east, higher in rural areas and lower in urban areas, and higher on the periphery and lower in the center”, which was highly consistent with the implementation of regional ecological restoration projects.

The land cover/use classification achieved an overall User’s Accuracy of 0.868 and Producer’s Accuracy of 0.859, with a Kappa coefficient of 0.886, verifying the reliability of the proposed method. The framework can effectively improve the refinement level of meso scale carbon sink estimation and enrich relevant data products and technical methods.

A key innovation of this study is that it balances the accuracy and efficiency of carbon storage estimation by integrating remote sensing inversion factors to correct carbon sequestration rates while retaining the advantages of the low-cost, easy-to-monitor “top-down” method, and enriches meso-scale carbon sink monitoring achievements by taking counties as the research object.

To further promote regional carbon neutrality, three recommendations are put forward:

1) strengthen long-term dynamic monitoring of carbon sinks in ecological restoration areas;

2) integrate higher-resolution remote sensing data to improve the accuracy of small-scale carbon sink assessment;

3) establish a standardized natural resource carbon sink database to support policy formulation for carbon trading and ecological compensation.

POLICY RECOMENDATIONS

Based on the results of natural resource carbon storage monitoring and spatiotemporal evolution analysis in the study area over the past 15 years, this paper proposes the following three policy recommendations:

First, strengthen the carbon sink orientation of territorial ecological restoration. During the delineation and implementation of the “Three Zones and Three Lines,” the spatial distribution characteristics of natural resource carbon sinks should be fully considered. Priority should be given to promoting ecological restoration and vegetation coverage enhancement projects in carbon sink cold spots (e.g., urban built-up areas, peripheries of townships), establishing carbon sink gradient management and control to enhance the overall carbon sink capacity of the region and the coordinated development level of “Production-Living-Ecological Spaces.” It is recommended that natural resource authorities introduce carbon sink spatial distribution layers as a key decision-making element in the implementation of territorial spatial planning and the dynamic assessment of the “Three Zones and Three Lines.” At the planning level, carbon sink cold spot areas (e.g., urban built-up area edges, industrial and mining concentrated zones with low carbon storage) should be prioritized for designation as key ecological restoration areas, with differentiated patch-level carbon sink enhancement targets set. At the project level, a “Carbon Sink Plus” ecological restoration model should be promoted. For instance, priority should be given to establishing high-efficiency mixed forests with strong carbon sink capacity around urban areas, and native carbon-sequestering plant species should be prioritized in the restoration of abandoned industrial and mining lands. Furthermore, a linkage mechanism should be established between carbon sink performance and policies regarding the allocation of restoration funds and the adjustment of land-use quotas.

Second, tailored to the characteristics of the study area, continuously promote wetland restoration and carbon sink value transformation in coal mining subsidence areas, and further explore integrating wetland carbon sinks into the ecological product value realization mechanism to strive for policy support from carbon sink trading and ecological compensation. Possible measures include: It is recommended that environmental and natural resource departments jointly lead the selection of typical subsidence wetlands to conduct research on baseline carbon sink surveys and monitoring methodology local standards (Ballantyne *et alii*, 2023), providing a compliant basis for carbon sink quantification. Promote the inclusion of certified wetland carbon sink projects into provincial and municipal pilot programs for ecological product value realization (GEP accounting) and carbon emission trading markets (e.g., CCER). Explore the “Eco-environment Oriented Development (EOD)” model, transforming future carbon sink revenue expectations into current financing capital for restoration and management to form a sustainable funding cycle. Concurrently, actively apply for provincial or national-level innovation pilot programs for ecological product value realization mechanisms to secure dedicated policy and financial support.

Third, promote the “Remote Sensing Correction+Land Parcel Classification” carbon sink monitoring technology system proposed in this study, and establish a regular county-level carbon sink accounting and dynamic assessment mechanism to provide a scientific basis for territorial spatial planning, ecological civilization construction assessment, and green high-quality development decision-making under the "dual carbon" goals. It is recommended that county-level governments take the lead, with the collaboration of natural resource departments, to localize and operationalize the "Remote Sensing Correction+Land Parcel Classification" technology system validated in this paper. This includes formulating a Technical Guideline for County-level Natural Resource Carbon Sink Monitoring and Assessment, establishing a regular accounting and dynamic updating platform integrating multi-source data, and deeply embedding carbon sink monitoring results into core management processes such as the compilation and implementation supervision of territorial spatial plans, the evaluation and assessment of ecological civilization construction targets, and the ecological impact assessment for site and route selection of key projects. By regularly publishing county-level carbon sink monitoring bulletins, quantitative, dynamic, and spatially visualized decision support can be provided for the disaggregation and assessment of "dual carbon" targets, horizontal transfer payments for ecological compensation, and the layout of green industry development.

FUNDING

This research was funded by Jiangsu Province Natural Resources Science and Technology Innovation Project under Grant JSZRKJ202409; Open Fund of Key Laboratory of Land Satellite Remote Sensing Applications, Ministry of Natural Resources under Grant KLSMNR-K202302; and 2023 Ministerial-Provincial Cooperation Pilot Project of the Ministry of Natural Resources under Grant 2023ZRBSHZ061.

REFERENCES

Anderson C. J. & Mitsch W. J. (2006) - *Sediment, carbon, and nutrient accumulation at two 10-year-old created riverine marshes*. Wetlands, **26**(3): 779-792.

Ballantyne A. P., Anderegg W. R. L. & Schimel D. et al. (2023) -*Toward a universal carbon cycle metric for evaluating anthropogenic sinks.* Environmental Research Letters, **18**: 034039.

Benoumeldjadj M., Boughouas S., Rached-Kanouni M. & Bouchareb A. (2025) - *Analyzing urbanization and environmental change in Aïn Fakroun, Algeria using landsat imagery through Google Earth Engine*. Italian Journal of Engineering Geology and Environment, **1**: 31-42.

Chen J. M., Ju W. M. & Ciais P. et al. (2022) - *Recent Progresses in Quantifying Carbon Budgets of Terrestrial Ecosystems at the Global-Regional Scale*. Remote Sensing of Environment, **269**: 112804.

Ghaderpour E., Bozzano F., Scarascia Mugnozza G. & Mazzanti P. (2025) - *Analyses of MODIS land cover/use and wildfires in italian regions since 2001*. Land, **14**(7): 1443.

Li Y., Zhang S., Wang J. & Liu, H. (2024) - *Impacts of climate and land-use change on fraction vegetation coverage based on PLUS-dimidiate pixel model.* Sustainability, 16(23), 10430.

Du M. D., Liu Y. & Cescatti A. et al. (2021) - *Satellite sun-induced chlorophyll fluorescence and near-infrared reflectance reveal complementary information on terrestrial gross primary production.* Remote Sensing of Environment, **255**: 112275.

Duan X.N., Wang X.K. & Lu F. et al. (2008) - *Carbon sequestration and its potential by wetland ecosystems in China*. Acta Ecologica Sinica, **28**(2): 463-469.

Fang J.Y., Piao S.L. & He J.S. et al. (2003) - *Increasing terrestrial vegetation activity in china over the last two decades*. Science in China Series C: Life Sciences, **33**(6): 554-565.

Fang J.Y., Yu G.R. & Liu L. L. et al. (2018) - *Climate change, human impacts, and carbon sequestration in China.* Proceedings of the National Academy of Sciences of the United States of America, **115**(16): 4015-4020.

Field C. B., Randerson J. T. & Malmström C. M. (1995) - *Global net primary production: combining ecology and remote sensing*. Remote Sensing of Environment, **51**(1): 74-88.

Gitelson A. A., et al. (2019) - *Remote Sensing of terrestrial primary productivity and carbon cycle: a review of the state of the art and future challenges.* Remote Sensing of Environment, **234**: 111445.

Gong P., Cheng X. & Fu H. H. et al. (2020) - *Remote sensing big data and artificial intelligence*. National Remote Sensing Bulletin, **24**(5): 507-515.

He J. N., Xiao Y. & Kang W. X. et al. (2015) - *Spatiotemporal dynamics of county-level forest carbon sinks in hunan province*. Acta Ecologica Sinica, **35**(18): 6115-6123.

Intergovernmental Panel on Climate Change (IPCC) (2018) - *Global Warming of 1.5°C: an IPCC Special Report.*

Jin Y. H., Liang B. L. & Guan T. et al. (2024) - *Analysis of the spatiotemporal evolution pattern of carbon budget at the county scale in Zhejiang Province*. Modern Urban Research, **10**: 27-28.

Li X. C., Ciais P. & Makowski D. et al. (2021) - *A global high-resolution map of soil organic carbon storage consistent with eddy-covariance fluxes*. Earth System Science Data, **13**: 1525-1546.

Li W. K., Macbean N. & Ciais P. et al. (2023) - *A global satellite-based vegetation index fusion product for fine-scale carbon cycle studies*. Earth System Science Data, **15**: 693-714.

Landis J. R. & Koch G. G. (1977) - *The measurement of observer agreement for categorical data.* Biometrics, **33**: 159-174.

Jung M., Reichstein M. & Margolis H. A. et al. (2011) - *Global patterns of land-atmosphere fluxes of carbon dioxide, latent heat, and sensible heat derived from eddy covariance, satellite, and meteorological observations*. Journal of Geophysical Research: Biogeosciences, **116**(G3): G00J07.

Liu L. Y. & Song B. W. (2022) - *Stereoscopic monitoring methods for terrestrial ecosystem carbon sequestration rate: progress and challenges.* Transactions of Atmospheric Sciences, **45**(3): 321-331.

Ministry of Ecology and Environment of the People's Republic of China, Research Center for Eco-Environmental Sciences, Chinese Academy of Sciences (2020) - *Technical guideline for Gross Ecosystem Product (GEP) accounting.* Beijing: Ministry of Ecology and Environment, **69**.

Ouyang Z. Y., Zhu C. Q. & Yang G.B. et al. (2013) - *Gross Ecosystem Product (GEP): concept, accounting framework and case study*. Acta Ecologica Sinica, **33**(21): 6747-6761.

Piao S. L., Fang J. Y. & Zhou L. M. et al. (2005) - *Changes in vegetation net primary productivity from 1982 to 1999 in China.* Global Biogeochemical Cycles, **19**(2): GB2027.

Sitch S., Friedlingstein P. & Gruber N. et al. (2023) - *Recent trends and drivers of global carbon sinks*. Global Biogeochemical Cycles, **37**: e2022GB007657.

Shen Z. B., Fang H. & He C. F. et al. (2024) - *Analysis of spatiotemporal changes of vegetation ecology and its meteorological driving forces in Zhenhai district from 2005 to 2021*. Geospatial Information, **22**(7): 80-83.

Sims D. A., Rahman A. F. & Cordova V. D. et al. (2008) - *A new model of gross primary productivity for north american ecosystems based solely on the enhanced vegetation index and land surface temperature from modis*. Remote Sensing of Environment, **112**(4): 1633-1646.

Wu C., Chen J. M. & Ni H. (2011) - *Predicting gross primary production from the enhanced vegetation index and photosynthetically active radiation: evaluation and calibration.* Remote Sensing of Environment, **115**(12): 3424-3435.

Wang Y. D., Wang X. K. & Lu F. et al. (2013) - *Research progress on carbon sink functions of Wetlands in China.* Acta Ecologica Sinica, **33**(17): 5141-5151.

Wang J. A., Zeng N. & Liu Y. L. et al. (2020) - *Towards monitoring the trajectory of the terrestrial carbon sink.* Nature Reviews Earth & Environment, **1**: 426-437.

Wang Y. P., Zhang H. Q. & Zhang Y. J. et al. (2022) - *Improving the MODIS GPP product for croplands by integrating the vpm model with high-resolution land-cover data*. Agricultural and Forest Meteorology, **323**: 108982.

Wang S. H., Zhang Y. G. & Ju W. M. et al. (2020) - *Tracking annual changes of carbon budget in china during 2001-2018 using Landsat and Sentinel data*. Science of the Total Environment, **723**: 137987.

Yuan W. P., Liu S. G. & Liu H. P. et al. (2022) - *Global comparison of light use efficiency models for simulating terrestrial vegetation gross primary production*. Remote Sensing, **14**: 597.

Yang W. D., Zeng L. B. & Li X. (2023) - *Research progress on carbon sink effects and their influencing factors*. Advances in Earth Science, **38**(2): 151-167.

Yu G. R., Zhu J. X. & Xu L. et al. (2022) - *Technological approaches for enhancing ecosystem carbon sink functions in China: nature-based solutions*. Bulletin of Chinese Academy of Sciences, **37**(4): 490-501.

Zhu X. W., Li D. Z. & Zhou S. H. et al. (2025) - *The policy framework, spatiotemporal characteristics, and policy recommendations for green and low-carbon development of chinese counties*. Modern Urban Research, **2**: 37.

Zhu L. W., Peng Y. F. & Chen C. et al. (2024) - *Research on cultivated land protection compensation from the perspective of carbon source and carbon sink*. Geospatial Information, **22**(12): 1-6.

Zhang H., Peng Q. R. & Wang R. et al. (2020) - *Spatiotemporal patterns and influencing factors of carbon sinks at the county level in China*. Acta Ecologica Sinica, **40**(24): 8988-8998.

Zhang B., Xie Z. X. & Gao J. X. (2021) - *Carbon sequestration function of shanghai urban forest vegetation and its effect on offsetting energy carbon emissions*. Acta Ecologica Sinica, **41**(22): 8906-8920.

Zhang X. Y., Zhang Y. J. & Zhu G. F. et al. (2023) - *A review of remote sensing approaches for monitoring wetland carbon dynamics.* Science of the Total Environment, **876**: 162818.

Zhang Y. Q., Zhang L. & Liu L. Y. et al. (2021) - *A consistent global modis vegetation index product for gross primary production estimation.* Remote Sensing of Environment, **258**: 112400.

Received November 2025 - Accepted March 2026